

Radar Signals Composed of Fragments With Square-Root and Linear Laws of Frequency Modulation

Kostyria O. O., Hryzo A. A., Varvarov V. V., Lukianchikov A. A., Drol O. Yu.

Ivan Kozhedub Kharkiv National Air Force University, Kharkiv, Ukraine

E-mail: oleksandr.kostyria@nure.ua

Application of digital waveform generation and signal processing technologies provides extensive opportunities for implementing radar probing pulses with various laws of frequency (phase) modulation (coding). With the introduction of linear frequency-modulated signals into radio engineering systems, research was initiated into reducing the peak level of side lobes in their autocorrelation functions, and this topic remains relevant today. One of the approaches to reducing this level is based on the use of signals with nonlinear frequency modulation composed of multiple segments. It has been established that, in order to avoid distortions in the resulting signal, it is necessary to introduce compensating terms that account for frequency-phase distortions at the first and subsequent junctions, as well as additional phase increments within the segments themselves, starting from the second segment. This study is devoted to the development of a new mathematical model of a three-segment signal consisting of a first segment with a square-root frequency modulation law and two subsequent segments with linear frequency modulation. Such a signal provides a reduction in the peak side lobe level compared to a classical linear frequency-modulated signal by 11.43 dB. A distinctive feature of the proposed mathematical model is the definition and incorporation of new compensating components into the expressions describing the second and third signal segments. The logic of the study determines the structure of the work. The first section is devoted to an analysis of existing publications, which indicates a lack of research in this direction, thereby confirming the relevance and necessity of the study, formulated in the second section. The third section provides a theoretical substantiation of the main principles – identifying the mechanisms of occurrence and deriving analytical expressions for compensating frequency-phase distortions arising at the first and second junctions, as well as within the second and third signal segments, for the case where the first segment has a nonlinear frequency modulation law and the subsequent two are linear. Further research is planned to focus on assessing the feasibility and features of combined application of spectral and time-domain window functions in radar signal processing.

Keywords: nonlinear frequency modulation; mathematical model; instantaneous frequency and phase discontinuity; autocorrelation function; maximum level of the side lobes

DOI: [10.64915/RADAP.2026.104.33-41](https://doi.org/10.64915/RADAP.2026.104.33-41)

Introduction

Experience in the use of radar technology under modern conditions demonstrates the necessity of performing tasks in a complex signal-interference environment, driven by the need to detect small-sized airborne targets at extremely low altitudes in the presence of intense clutter from local objects. Under such conditions, the problem of minimizing the Maximum Level of the Side Lobes (MLSL) of the Autocorrelation Functions (ACF) of probing signals is of critical importance. In this context, complex waveforms are widely used, whose time – bandwidth product (i.e., the signal base), defined as the product of pulse duration and signal bandwidth, is given as $B = T_s \cdot \Delta f > 1$ [1–9].

One of the promising methods for reducing the MLSL is the use of signals with Nonlinear Frequency Modulation (NLFM), which are formed by combining several segments (two or more) with identical or different Frequency Modulation (FM) laws. In this case, the FM Rate (FMR) at one or both edges of the signal is somewhat higher, resulting in unilateral or bilateral smoothing of its Amplitude-Frequency Spectrum (AFS) [3–7], which is equivalent to applying weighted (window) processing in the time domain [6–13].

The results obtained in [14–20] demonstrated that in multi-segment NLFM signals, frequency-phase distortions may arise both at the junctions and within the segments following them, i.e., in the second and subsequent segments. The occurrence of such di-

scontinuities leads to distortion of the oscillogram and the AFS of the resulting signal and, consequently, may result in an increase in the MLSL of ACF. To compensate for such frequency-phase distortions, compensating terms are introduced into the description of the instantaneous phase and frequency of the signals when using Mathematical Models (MM) in continuous time, or only into the phase description in the case of time-shifted MM.

It is evident that smooth shaping of the AFS provides better MLSL reduction performance, therefore, it is desirable to ensure a nonlinear variation of the FMR at the edges of the AFS. However, in this case, the process of determining compensating terms for seamless stitching of segments becomes more complex, since their FMR laws differ, and the FMR of preceding segments induces additional phase increments in all subsequent segments [14].

In this context, the present work investigates the possibility of seamless stitching of a segment with nonlinear FM with two subsequent segments having linear FM, with a gradual increase in the FMR.

1 Analysis of Research and Publications

The development of radar signals with intra-pulse frequency (phase) modulation, also referred to as complex signals, has laid the foundation for the widespread implementation of solid-state radar transmitters and the creation of active phased array antennas, which are now the basis for constructing radio-technical systems of various purposes [1–9]. Complex probing signals make it possible to ensure the required power of the probing pulse by increasing its duration, while subsequent pulse compression in a matched filter allows achieving the desired range resolution.

The main drawback of complex signals is the relatively high MLSL of their ACF, which generates additional clutter in the presence of reflections from local objects and masks echo-signals from small airborne targets when strong targets with large radar cross-sections are present nearby [1–9, 15].

The relevance of the problem of further MLSL reduction has remained high for many decades. To address it, the use of NLFM signals has been proposed by the authors in [7, 14–43]. Historically, NLFM signals were first introduced in air surveillance systems [3, 4, 6–30], and research in this area continues actively [13, 31–40]. For this purpose, NLFM signals based on both Linear Frequency Modulation (LFM) and NLFM fragments have been proposed in [14, 16, 18–20, 22, 25–27, 30, 33–35]. In studies [14, 16, 18–20, 27], the characteristics of such signals were compared with those of the classical LFM signal. The LFM signal was selected as the baseline model for comparison because it is the most widespread and commonly accepted

waveform in radar practice [1–9], thereby enabling consistent comparison of results from different studies with respect to a unified reference signal.

The development of cognitive radars has driven studies of the impact of Doppler frequency on echo-signal processing results in radar systems employing NLFM signals [41–43]. The problem of ensuring electromagnetic compatibility between both like-type and different-type radio-technical systems also remains relevant, for which a set of measures is proposed [44–47] aimed at controlling and reducing out-of-band emissions.

Research on the implementation of NLFM signals in radio-technical systems is focused on the development of new and improvement of existing MM, considering both single-segment [6, 21–24] and multi-segment [7, 14–20, 22, 25–28] configurations.

A distinctive feature of [14–20] is that the developed MM of NLFM signals include terms compensating for instantaneous frequency and phase discontinuities at segment junctions, as well as additional phase increments within the segments themselves, which ensures a reduction in the MLSL of the ACF of such signals. MM of an NLFM signal composed of a Square-Root Frequency Modulation (SQFM) segment and a LFM segment [16], as well as a signal composed of three LFM segments [18], have already been studied.

The conducted analysis shows that a signal consisting of an initial SQFM segment followed by two LFM segments has not been investigated in the context of compensation of the resulting frequency-phase distortions in existing studies.

2 Formulation of the research task

The aim of the work is to reduce the MLSL of the ACF of radar signals by introducing an NLFM signal based on a new MM in continuous time. In contrast to the already developed MM of three-segment signals with LFM segments, the introduction of a nonlinear FM segment necessitates deriving new expressions for calculating compensating components of frequency-phase distortions that arise at the junctions and within the segments themselves.

Achieving the objective of developing a new MM involves the following interrelated subtasks:

- determining the specific features of the processes of formation and compensation of frequency and phase distortions in the MM in continuous time of NLFM signals whose segments have heterogeneous FM laws;
- developing an MM in continuous time of an NLFM signal formed by the sequential concatenation of a SQFM segment and two linear FM segments, i.e., a SQFM–LFM–LFM signal;

- analytically investigating the characteristics of frequency-phase distortion formation at the junctions between segments in the SQFM-LFM-LFM signal;
- deriving mathematical expressions for the SQFM-LFM-LFM signal describing compensating components of instantaneous frequency and phase distortions arising at the junctions and within the segments, starting from the second segment;
- studying the new MM through comparative analysis of results obtained using it and data from existing sources or previously developed similar MM;
- verifying the validity of the obtained results through analysis of graphical materials confirming the achievement of the stated objective.

The sequential implementation of the formulated tasks ensures a step-by-step realization of the research objective – reduction of the MLSL of ACF of NLFM signals by combining different-type segments and compensating for the resulting frequency-phase distortions.

3 Description of the Research Material

3.1 Features of the occurrence and compensation of frequency-phase distortions in the continuous-time MM of an NLFM signal in the presence of segments with different FM laws

In [14–20], it was shown that frequency and phase discontinuities may occur at the junctions of NLFM signal segments, caused by changes in values or the emergence of a new higher-order derivative of the instantaneous phase at the moments of switching the FM law.

The most extensively studied are NLFM signals composed of LFM segments [18, 25, 26, 28]. In this case, the absence of phase discontinuities can be ensured by generating an integer number of radio-frequency oscillation periods within each segment, which guarantees identical zero values of the instantaneous phase at their junctions [17]. This case is a particular one, in general, the phase values at segment boundaries are nonzero and different, which leads to the occurrence of discontinuities.

In [14], it was shown that when transitioning to each subsequent segment, it is necessary to account for the impact of instantaneous phase discontinuities that arise at all previous segment junctions. The study was

performed for an MM of an NLFM signal composed of five LFM segments; however, this property manifests itself regardless of changes in the FM law of the segments.

Taking the above into account, let us formulate the features of MM synthesis for multi-segment NLFM signals composed of segments with different FM laws.

The main source of frequency-phase distortions in the MM of multi-segment NLFM signals is the instantaneous phase discontinuities at the moments of transition from one segment to another, which cause a stepwise change in frequency:

$$\delta f_n = \frac{\delta \varphi_n}{dt} \quad (1)$$

and the magnitude of the phase discontinuity is determined as the difference between the initial phase φ_{Sn} of the subsequent n -th segment and the final phase of the previous $n-1$ segment φ_{En-1} :

$$\delta \varphi_n = \varphi_{Sn} - \varphi_{En-1}. \quad (2)$$

Frequency-phase distortions at segment junctions also manifest themselves as additional phase increments in all subsequent segments, and neglecting these increments leads to an increase in the frequency deviation of these segments. In other words, if during the synthesis an NLFM signal is obtained with a frequency deviation higher than the specified one, despite compensation of frequency and phase discontinuities, this indicates that such additional phase increments have not been taken into account.

These features are general for multi-segment NLFM signals for any combination of FM laws in the segments, therefore, they are applied to the development of a continuous-time MM with square-root and linear FM laws, and the obtained results are compared with simulation results of a classical LFM signal and a previously developed LFM-LFM-LFM signal with identical time-frequency parameters.

3.2 Synthesis of a continuous-time MM of a three-segment NLFM signal of the SQFM-LFM-LFM type

As initial models, we use the MM of a two-segment NLFM signal SQFM-LFM [16] and the three-segment LFM-LFM-LFM signal [18]. Taking into account the previously discussed features, the new MM of the three-segment signal cannot be obtained by a direct combination of the two mentioned MM, since frequency-phase distortions at the junction between the SQFM and LFM segments will manifest themselves in the third LFM segment.

Let us consider in detail the continuous-time MM of the two-segment NLFM signal SQFM-LFM, proposed in [16].

In the general case, the FMR of the first, i.e., SQFM, segment varies in time:

$$\beta_1(t) = \frac{\beta_{1M}}{2} \sqrt{\frac{T_1}{t}}, \quad (3)$$

where β_{1M} – the average FMR of the segment, which is determined by the following relation:

$$\beta_{1M} = \frac{\Delta f_1}{T_1},$$

where T_n – duration of the n -th signal segment ($n=1,2,3$); Δf_n – frequency deviation of the n -th segment.

For the time instant $t=T_1$, the value of the FMR (3) is equal to:

$$\beta_1(T_1) = \beta_{E1} = \frac{\beta_{1M}}{2}. \quad (4)$$

Based on (4), the final phase of the first segment is given by:

$$\varphi_{E1} = 2\pi \left(f_0 T_1 + \frac{1}{3} \beta_{1M} T_1^2 \right), \quad (5)$$

where f_0 is the initial frequency of the NLFM signal.

The initial phase of the second segment is determined as:

$$\varphi_{S2} = 2\pi \left(f_0 T_1 + \frac{1}{2} \beta_2 T_1^2 \right), \quad (6)$$

where β_2 – the FMR of the 2-th segment:

$$\beta_2 = \frac{\Delta f_2}{T_2}.$$

Taking into account (5) and (6), the value of the phase discontinuity at the junction of the first and second segments is obtained as:

$$\delta\varphi_{12} = 2\pi T_1^2 \left(\frac{\beta_2}{2} - \frac{\beta_{1M}}{3} \right), \quad (7)$$

the frequency discontinuity is determined as:

$$\delta f_{12} = T_1(\beta_2 - \beta_{1M}), \quad (8)$$

which, in turn, causes an additional phase increment in the second segment that requires compensation. By introducing a compensating term, we obtain the MM of the signal with a first SQFM segment and a second LFM segment:

$$\varphi(t) = \begin{cases} 2\pi \left[f_0 t + \frac{2\beta_{1M}\sqrt{t^3 T_1}}{3} \right], & 0 \leq t \leq T_1; \\ 2\pi \left[(f_0 + \Delta f_1 - \beta_2 T_1)t + \frac{\beta_2 t^2}{2} \right] - \delta\varphi_{12}, & T_1 < t \leq T_1 + T_2. \end{cases} \quad (9)$$

In the next step, we refine the expression for the third LFM segment, using the results obtained in [18]

for the MM of a three-segment NLFM signal of the LFM-LFM-LFM type:

$$\varphi(t) = \begin{cases} 2\pi \left\{ f_0 t + \frac{\beta_1 t^2}{2} \right\}, & 0 \leq t \leq T_1; \\ 2\pi \left\{ [f_0 - (\beta_2 - \beta_1)T_1]t + \frac{\beta_2 t^2}{2} \right\} - \delta\varphi_{12}, & T_1 < t \leq T_1 + T_2; \\ 2\pi \left\{ [f_0 - (\beta_3 - \beta_1)T_1 - (\beta_3 - \beta_2)T_2]t + \frac{\beta_3 t^2}{2} \right\} - \delta\varphi_{23}, & T_1 + T_2 < t \leq T_S, \end{cases} \quad (10)$$

where $T_S = T_1 + T_2 + T_3$; β_3 – the FMR of the 3-th segment:

$$\beta_3 = \frac{\Delta f_3}{T_3}.$$

Finally, taking into account (9) and (10), we introduce a new MM of the NLFM signal of the SQFM-LFM-LFM type:

$$\varphi(t) = \begin{cases} 2\pi \left\{ f_0 t + \frac{2\beta_{1M}\sqrt{t^3 T_1}}{3} \right\}, & 0 \leq t \leq T_1; \\ 2\pi \left\{ [f_0 - (\beta_2 - \beta_{1M})T_1]t + \frac{\beta_2 t^2}{2} \right\} - \delta\varphi_{12}, & T_1 < t \leq T_1 + T_2; \\ 2\pi \left\{ [f_0 - (\beta_3 - \beta_{1M})T_1 - (\beta_3 - \beta_2)T_2]t + \frac{\beta_3 t^2}{2} \right\} \pm \delta\varphi_{12} \pm \delta\varphi_{23}, & T_1 + T_2 < t \leq T_S. \end{cases} \quad (11)$$

In (11), the value of $\delta\varphi_{12}$ is calculated in accordance with (7), and $\delta\varphi_{23}$ is determined by the expression:

$$\delta\varphi_{23} = 2\pi \left\{ (\beta_3 - \beta_2) \cdot \left(T_1 + \frac{1}{2}T_2 \right) T_2 + \left(\beta_2 - \frac{\beta_{1M}}{2} \right) T_1^2 \right\}. \quad (12)$$

which is obtained using (2).

It should be noted that, to determine the instantaneous phase of the third segment, the phase discontinuity at the previous junction between the first and second segments must be taken into account, which is fully justified. It should also be emphasized that, at the beginning of the third segment, phase drift may reach large values, and the final phase of the previous segment and the initial phase of the subsequent segment may lie in different phase quadrants, which must be accounted for. In other words, when varying the time-frequency parameters of the NLFM signal in (11), it may be necessary to select the signs for $\delta\varphi_{12}$, $\delta\varphi_{23}$ as appropriate, both in the absence and in the presence of a compensating π -discontinuity.

3.3 Results of mathematical modeling

To verify the validity of the proposed MM (11), a comparative was performed in MATLAB between the results obtained using this model and those obtained using the classical LFM signal MM [7] and the NLFM signal of the LFM-LFM-LFM type [18], under identical frequency deviations and pulse durations of the signals. The following parameters were compared:

- MLSL of the ACF;
- sidelobe decay rate of the ACF;
- Main Lobe (ML) width of the ACF at the 0.707 level.

The selected time-frequency parameters of the signals and the obtained values of their ACF characteristics are summarized in Table 1.

Табл. 1 Results of the study of MM LFM and NLFM signals of the LFM-LFM-LFM and SQFM-LFM-LFM types

Signal type	T_1 , μs	T_2 , μs	T_3 , μs	Δf_1 , kHz	Δf_2 , kHz	Δf_3 , kHz	MLSL, dB	Sidelobe decay rate, dB/dec	ML ACF (0.707), μs
LFM	160*	160*	160*	160*	500*	500*	-13.42*	19.98*	1.76*
	160	160	160	160	1000	1000	-13.34	20.06	0.88
	200	200	200	200	500	500	-13.39	19.86	1.764
	200	200	200	200	1000	1000	-13.35	19.85	0.882
	240	240	240	240	500	500	-13.44	19.6	1.77
	240	240	240	240	1000	1000	-13.44	19.6	0.885
	260	260	260	260	500	500	-13.33	19.7	1.774
LFM-LFM-LFM	20*	120*	20*	100*	300*	100*	-18.95*	16.8*	2.05*
	20	120	20	200	600	200	-19.32	17.7	1.025
	25	150	25	100	300	100	-19.1	18.5	2.05
	25	150	25	200	600	200	-19.4	19.35	1.025
	30	180	30	100	300	100	-19.2	18.5	2.048
	30	180	30	200	600	200	-19.46	18.5	1.024
	20	220	20	100	300	100	-19.09	17.9	2.31
SQFM-LFM-LFM	40*	80*	40*	200*	100*	200*	-24.85*	27.0*	2.56*
	40	80	40	400	200	400	-23.31	25.32	1.28
	40	120	40	200	100	200	-22.17	22.11	2.9
	40	120	40	400	200	400	-20.52	26.62	1.45
	40	160	40	200	100	200	-20.21	21.2	2.69
	40	160	40	400	200	400	-18.96	29.41	1.34
	40	180	40	200	100	200	-20.37	25.22	3.39
	40	180	40	400	200	400	-18.4	30.43	1.68

*Values marked with * are used for further comparative analysis.*

Comparative analysis of the data in Table 1 shows that, for the selected time-frequency parameters of LFM and NLFM signals, the use of the proposed SQFM-LFM-LFM type signals provides:

- a reduction of the MLSL relative to the LFM signal by an average of 7.72 dB, with a maximum reduction for signals with equivalent time-frequency parameters of 11.43 dB;
- a reduction of the MLSL relative to the NLFM signal of the LFM-LFM-LFM type by an average of 1.82 dB, while the maximum reduction under identical time-frequency parameters reaches 5.9 dB;

- the highest value of the ACF sidelobe decay rate, which on average equals 25.9 dB/dec;
- an increase in the ACF ML width at the 0.707 level relative to the LFM signal by 45.5%, and relative to the three-segment NLFM signal based on LFM elements by 25%.

The simulation results are confirmed by graphical material, which clearly demonstrates the validity of the obtained results.

Figures 1a and 2a show the plots of the instantaneous frequency variation of the studied LFM-LFM-LFM and SQFM-LFM-LFM signals, respectively.

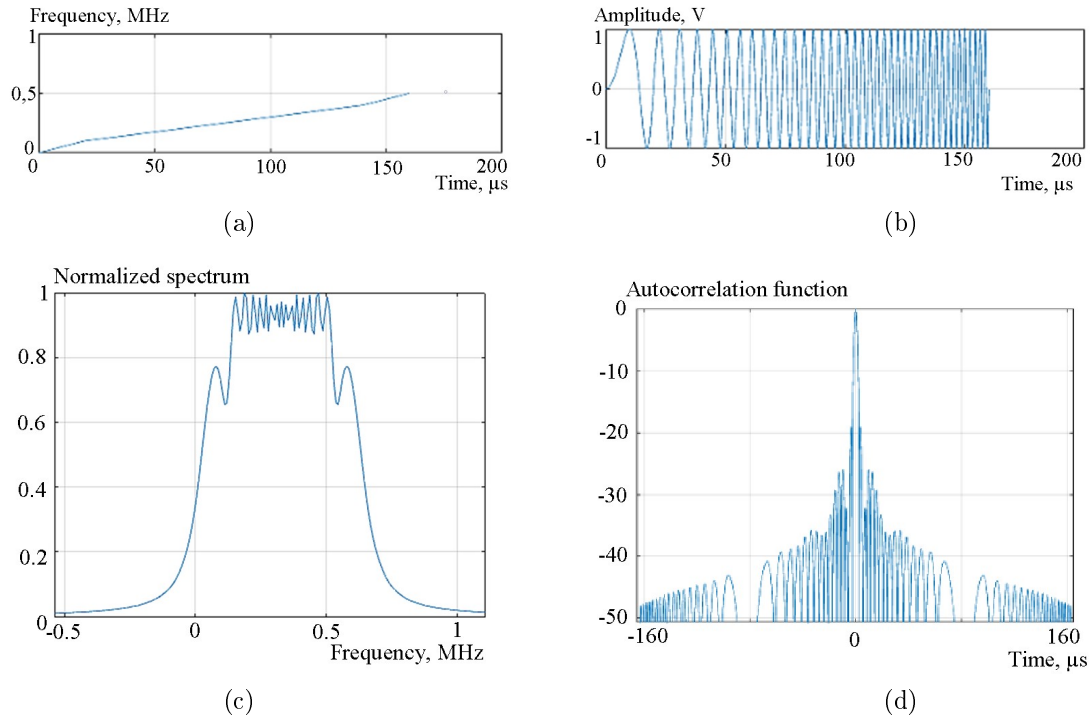


Fig. 1. Plot of instantaneous frequency variation (a), oscillogram (b), AFS (c), ACF (d) of the LFM-LFM-LFM signal

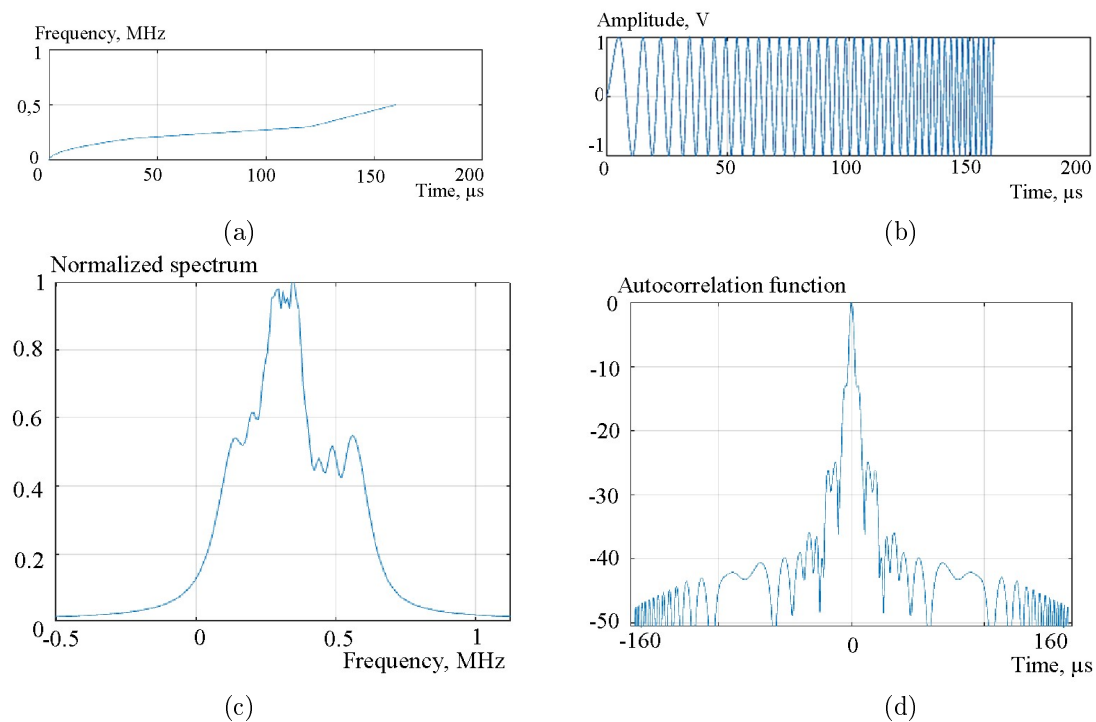


Fig. 2. Plot of instantaneous frequency variation (a), oscillogram (b), AFS (c), ACF (d) of the SQFM-LFM-LFM signal

The frequency variation laws, segment durations, total frequency deviations, and signal durations correspond to the specified values. These parameters are marked with “*” in Table 1.

The oscillograms in Figs. 1b and 2b demonstrate a smooth frequency increase of the signals and the absence of phase discontinuities at the segment junctions, which is confirmed by the shape of their AFS in Figs. 1c and 2c. The presented AFS do not exhibit

dips or discontinuities at the segment junctions, and no additional ripples on their slopes and “wings” are observed.

The ACF plots in Figs. 1d and 2d require a more detailed analysis. For the NLFM signal composed of three LFM segments, the ACF shape is close to that of a classical LFM signal. The introduction of additional segments leads to a redistribution of energy among the sidelobes, which results in a reduction of the near sidelobe levels, while the ML becomes slightly wider. A reduction in the MLSL relative to the single-segment LFM signal is observed (the corresponding row in Table 1 is marked with “*”), which for this set of time-frequency parameters equals -18.96 dB. At the same time, a moderate broadening of the ML is observed.

As a result of introducing the SQFM segment, the ACF shown in Fig. 2d for the specified NLFM signal parameters exhibits a merging of the ML and the near sidelobes, resulting in a pedestal at approximately -13 dB. The ML also becomes wider; however, the MLSL decreases to -24.85 dB, which represents the lowest value obtained in this study.

Conclusions

In this work, a new continuous-time MM of an NLFM signal has been developed, consisting of a SQFM segment and two LFM segments. A distinctive feature of the proposed MM is the calculation and introduction of compensating terms that eliminate frequency and phase discontinuities occurring at segment junctions due to changes in the FMR when transitioning to a new segment, as well as additional phase increments in the segments following the junctions.

The synthesis features of multi-segment NLFM signals containing segments with both identical and different FM laws have been formulated. The primary source of frequency-phase distortion in such signals is identified as instantaneous phase discontinuities at segment junctions, which in turn cause frequency jumps. In the continuous-time MM, frequency-phase distortions at segment junctions manifest as additional phase increments in subsequent segments; neglecting them increases frequency deviation and leads to a mismatch between the signals and the specified parameters.

With a PSL reduction of 11.43 dB (by 85%) compared to the conventional LFM signal, the ML width of the ACF for the proposed signal increases by 45.5%, which represents an acceptable trade-off for target detection tasks under conditions of intense clutter interference from local objects.

The results of mathematical modeling confirmed the feasibility of applying the proposed signal in practi-

ce. The introduction of the SQFM segment significantly reduces the MLSL of the resulting signal ACF and increases the sidelobe decay rate.

The increase in the ML width of SQFM-LFM-LFM signals limits time and frequency resolution. For practical applications, optimal signal parameters should be determined in the Pareto sense, ensuring a balance between MLSL and allowable ML width.

The obtained results may be used by specialists working in the field of further MLSL reduction in radar signals. In addition, the proposed NLFM signal expands the set of complex probing waveforms, contributing to improved resistance to electronic countermeasures and electromagnetic compatibility of radar systems.

Future work will focus on investigating the feasibility and effectiveness of combined spectral and time-domain windowing for MLSL reduction and identifying the corresponding implementation features.

References

- [1] Blackman S. S., and Popoli R. F. (1990). *Design and Analysis of Modern Tracking Systems*. Boston, London: Artech House, 1230 p.
- [2] McDonough R. N., and Whalen A. D. (1995). *Detection of Signals in Noise* (2nd. ed.). San Diego: Academic Press, Inc., USA, 495 p.
- [3] Richards M. A., Scheer J. A., Holm W. A. (2010). *Principles of modern radar, Vol. I: Basic Principles*. Chelsea: Sheridan Books, Inc., 962 p.
- [4] Melvin W. L., and Scheer J. A. (2013). *Principles of Modern Radar. Vol. II: Advanced techniques*. Sci Tech Publishing, 846 p.
- [5] Van Trees H. L. (2001). *Detection, Estimation, and Modulation Theory, Part III: Radar-Sonar Processing and Gaussian Signals in Noise*. John Wiley & Sons, Inc., 643 p.
- [6] Skolnik M. I. (1981). *Introduction to Radar Systems. Second Edition*. Singapore: McGraw-Hill Book Co., 581 p.
- [7] Cook C. E., and Bernfeld M. (1993). *Radar Signals: An Introduction to Theory and Application*. Artech House, 552 p.
- [8] Barton D. K. (2004). *Radar System Analysis and Modeling*. Boston, London: Artech House Publishers, 566 p.
- [9] Levanon N., and Mozeson E. (2004). *Radar Signals*. John Wiley & Sons, 432 p. DOI: 10.1002/0471663085.
- [10] Doerry A. W. (2017). *Catalog of Window Taper Functions for Sidelobe Control. Technical Report SAND2017-4042*. Sandia National Labs., USA, 208 p. DOI: 10.2172/1365510.
- [11] Adithya Valli N., Elizabeth Rani D., & Kavitha C. (2021). Study on Conventional vs. Convolutional Windows for Reduction of Side Lobes. *Recent Developments in Engineering Research*, Vol. 12, pp. 159–167. DOI: 10.9734/bpi/rder/v12/5076D

- [12] Muralidhara N., Velayudhan V., and Kumar M. (2022). Performance Analysis of Weighing Functions for Radar Target Detection. *International Journal of Engineering Research & Technology (IJERT)*, Vol. 11, Iss. 03, pp. 161-165. DOI: 10.17577/IJERTV11IS030044.
- [13] Zhang Y., Wang W., Wang R., et al. (2020). A Novel NLFM Waveform with Low Sidelobes Based on Modified Chebyshev Window. *IEEE Geosci. Remote Sens. Lett.*, Vol. 17, Iss. 5, pp. 814-818. DOI: 10.1109/LGRS.2019.2930817.
- [14] Kostyria O. O., Hryzo A. A., Fedorov A. V., et al. (2025). Mathematical Model of the Current Time of a Five Fragment Nonlinear Frequency Modulated Signal. *Advances in Military Technology*, Vol. 20(2), pp. 435-447. DOI: 10.3849/aimt.01986.
- [15] Kostyria O. O., Hryzo A. A., Fedorov A. V., et al. (2025). Assessment of the Quality of Detection of a radar Signal with Nonlinear Frequency Modulation in the Presence of a non-stationary Interfering Background. *Radio Electronics, Computer Science, Control*, Vol. 1(72), pp. 18-29. DOI: 10.15588/1607-3274-2025-1-2.
- [16] Kostyria, O. O., Hryzo, A. A., Khudov V. H., et al. (2024). Two-Fragment Non-Linear-Frequency Modulated Signals with Roots of Quadratic and Linear Laws Frequency Changes. *Radio Electronics, Computer Science, Control*, Vol. 1(68), pp. 17-27. DOI: 10.15588/1607-3274-2024-1-2.
- [17] Kostyria O. O., Hryzo A. A., Dodukh O. M., et al. (2023). Method of Minimization Sidelobes Level Autocorrelation Functions of Signals with Non-Linear Frequency Modulation. *Radio Electronics, Computer Science, Control*, Vol. 4(67), pp. 39-48. DOI: 10.15588/1607-3274-2023-4-4.
- [18] Kostyria O. O., Hryzo A. A., Dodukh O. M., et al. (2023). Mathematical Model of the Current Time for Three-Fragment Radar Signal with Nonlinear Frequency Modulation. *Radio Electronics, Computer Science, Control*, Vol. 3(63), pp. 17-26. DOI: 10.15588/1607-3274-2023-3-2.
- [19] Kostyria, O. O., Hryzo, A. A., Khudov V. H., et al. (2024). Mathematical Model of Current Time of Signal from Serial Combination Linear-Frequency and Quadratically Modulated Fragments. *Radio Electronics, Computer Science, Control*, Vol. 2(69), pp. 24-33. DOI: 10.15588/1607-3274-2024-2-2.
- [20] Kostyria O. O., Hryzo A. A., and Dodukh O. M. (2023). Compensation for distortions of the frequency-time structure of the combined signal under the condition of different number of derivatives of the instantaneous phase of its fragments. *Scientific Works of Kharkiv National Air Force University*, Vol. 4 (78), pp. 70-75. DOI: 10.30748/zhups.2023.78.10.
- [21] Hemmingsen D. M., McCormick P. M., Blunt S. D., et al. (2018). Waveform-Diverse stretch Processing. *2018 IEEE Radar Conference (RadarConf18)*, pp. 0963-0968. DOI: 10.1109/RADAR.2018.8378691.
- [22] Xu Z., Wang X., Wang Y. (2022). Nonlinear Frequency Modulated Waveforms Modeling and Optimization for Radar Applications. *Mathematics*, Vol. 10(21), Article id. 3939, pp. 1-11. DOI: 10.3390/math10213939.
- [23] Zhang Y., Deng Y., Zhang Z., et al. (2022). Parametric NLFM Waveform for Space-borne Synthetic Aperture Radar. *IEEE Transactions on Geoscience and Remote Sensing*, Vol. 60, pp. 1-9, Article no. 5238909. DOI: 10.1109/TGRS.2022.3221433.
- [24] Collins T., Atkins P. (1999). Nonlinear Frequency Modulation Chirps for active Sonar. *IEEE Proc. Radar Sonar Navig.*, 146(6), pp. 312-316. DOI: 10.1049/ip-rsn:19990754.
- [25] Septanto H., Sudjana O., and Suprijanto D. (2022). A Novel Rule for Designing Tri-Stages Piecewise Linear NLFM Chirp. *2022 International Conference on Radar, Antenna, Microwave, Electronics, and Telecommunications (ICRAMET)*, Indonesia, IEEE, pp. 62-67. DOI: 10.1109/ICRAMET56917.2022.9991201.
- [26] Saleh M., Omar S.-M., Grivel E., et al. (2021). A Variable Chirp Rate Stepped Frequency Linear Frequency Modulation Waveform Designed to Approximate Wideband Non-Linear Radar Waveforms. *Digital Signal Processing*, Vol. 109, Article id. 102884. DOI: 10.1016/j.dsp.2020.102884.
- [27] Parwana S., Kumar S. (2015). Analysis of LFM and NLFM Radar Waveforms and their Performance Analysis. *International Research Journal of Engineering and Technology (IRJET)*, Vol. 02, Iss. 02, pp. 334-339.
- [28] Valli N. A., Rani D. E., Kavitha C. (2019). Modified Radar Signal Model using NLFM. *International Journal of Recent Technology and Engineering (IJRTE)*, Vol. 8, Iss. 2S3, pp. 513-516. DOI: 10.35940/ijrte.B1091.0782S319.
- [29] Wang, G., Wu, J., Sun, Y., et al. (2022). Digital Compensation Technique for Wideband Phased Array Radar Using Nonlinear Frequency Modulation. *2022 IEEE 22nd International Conference on Communication Technology, ICCT 2022*, pp. 639-644. DOI: 10.1109/ICCT56141.2022.10073280.
- [30] Zhuang R., Fan H., Sun Y., et al. (2021). Pulse-Agile Waveform Design for Nonlinear FM Pulses Based on Spectrum Modulation. *IET International Radar Conference (IET IRC 2020), Online Conference*, pp. 964-969. DOI: 10.1049/icp.2021.0700.
- [31] Xu W., Zhang L., Fang C., et al. (2021). Staring Spotlight SAR with Nonlinear Frequency Modulation Signal and Azimuth Non-Uniform Sampling for Low Sidelobe Imaging. *Sensors*, Vol. 21(19), Article no. 6487. DOI: 10.3390/s21196487.
- [32] Chan Y. K., Chua M. Y., and Koo V. C. (2009). Side Lobes Reduction using Simple Two and Tri-Stages Nonlinear Frequency Modulation (NLFM). *Progress in Electromagnetics Research, (PIER)*, Vol. 98, pp. 33-52. DOI: 10.2528/PIER09073004.
- [33] Ghavamirad J. R., Sadeghzadeh R.A., Sebt M. A. (2025). Sidelobe Level Reduction in the ACF of NLFM Signals Using the Smoothing Spline Method. *Electrical Engineering and Systems Science, Signal Processing: arXiv:2501.06657 [eess.SP]*, 5 p. DOI: 10.48550/arXiv.2501.06657.
- [34] Ch Anoosha and Krishna B.T. (2022). Peak Sidelobe Reduction analysis of NLFM and Improved NLFM Radar signal with Non-Uniform PRI. *Aiub Journal of Science and Engineering (AJSE)*, Vol. 21, Iss. 2, pp. 125-131. DOI: 10.53799/ajse.v21i2.440.
- [35] Wei T., Wang W., Zhang Y., et al. (2022). Novel Nonlinear Frequency Modulation Waveform with Low Sidelobes Applied to Synthetic Aperture Radar. *IEEE Geoscience and Remote Sensing Letters*, Vol. 19, pp. 1-5, 2022, Art no. 4515405. DOI: 10.1109/LGRS.2022.3216340.
- [36] Jin G., Deng Y., Wang R., et al. (2019). An Advanced Nonlinear Frequency Modulation Waveform for Radar Imaging with Low Sidelobe. *IEEE Transactions on Geoscience and Remote Sensing*, Vol. 57, Iss. 8, pp. 6155-6168. DOI: 10.1109/TGRS.2019.2904627.

- [37] Roy A., Nemade H. B., Bhattacharjee R. (2021). Radar Waveform Diversity using Nonlinear Chirp with Improved Sidelobe Level Performance. *AEU – International Journal of Electronics and Communications*, Vol. 136, Article id. 153768. DOI: 10.1016/J.AEUE.2021.153768.
- [38] Sankuru S. P., Babu P., and Alaae-Kerahroodi M. (2022). UNIPOL: Unimodular sequence Design via a Separable iterative Quartic Polynomial Optimization for Active sensing Systems. *Signal Processing*, Vol. 190, Article no 108348. DOI: 10.1016/j.sigpro.2021.108348.
- [39] Jyothi R., Babu P., and Alaae-Kerahroodi M. (2021). Slope: A Monotonic Algorithm to Design Sequences with good Autocorrelation Properties by Minimizing the Peak Sidelobe Level. *Digital Signal Processing*, Vol. 116, Article no 103142. DOI: 10.1016/j.dsp.2021.103142.
- [40] Sankuru S. P., Jyothi R., Babu P., et al. (2021). Designing Sequence set with Minimal Peak Side-Lobe Level for Applications in high Resolution Radar Imaging. *IEEE Open Journal of Signal Processing*, Vol. 2, pp. 17–32. DOI: 10.48550/arXiv.2009.03081.
- [41] Valli N. A., Rani D. E., Kavitha C. (2019). Doppler Effect Analysis of NLFM Signals. *International Journal of Scientific & Technology Research*, Vol. 8, Iss. 11, pp. 1817–1821.
- [42] Ping T., Song C., Qi Z., et al. (2024). PHS: A Pulse Sequence Method Based on Hyperbolic Frequency Modulation for Speed Measurement. *International Journal of Distributed Sensor Networks*, Vol. 2024, Article no 6670576, 11 p. DOI: 10.1155/2024/6670576.
- [43] Adithya Valli N., Elizabeth Rani D., Kavitha C. (2020). Performance Analysis of NLFM Signals with Doppler Effect and Background Noise. *International Journal of Engineering and Advanced Technology (IJEAT)*, Vol. 9, Iss. 3, pp. 737–742. DOI: 10.35940/ijeat.B3835.029320.
- [44] Alaae-Kerahroodi M., Raei E., Kumar S., et al. (2022). Cognitive Radar Waveform Design and Prototype for Coexistence with Communications. *IEEE Sensors Journal*, Vol. 22, Iss. 10, pp. 9787–9802. DOI: 10.1109/jsen.2022.3163548.
- [45] Aubry A., De Maio A., Govoni M. A., et al. (2020). On the Design of Multi-Spectrally Constrained Constant Modulus Radar Signals. *IEEE Transactions on Signal Processing*, Vol. 68, pp. 2231–2243. DOI: 10.1109/tsp.2020.2983642.
- [46] Martone F., Sherbondy K. D., Kovarskiy J. A., et al. (2021). Closing the Loop on Cognitive Radar for Spectrum Sharing. *IEEE Aerospace and Electronic Systems Magazine*, Vol. 36, no. 9, pp. 44–55. DOI: 10.1109/MAES.2021.3072698.
- [47] Yang J., Aubry A., De Maio A., et al. (2020). Design of Constant Modulus Discrete Phase Radar Waveforms Subject to Multi-Spectral Constraints. *IEEE Signal Processing Letters*, Vol. 27, pp. 875–879. DOI: 10.1109/LSP.2020.2991357.

Радіолокаційні сигнали у складі фрагментів з корінь-квадратичним та лінійними законами частотної модуляції

Костиця О. О., Гризо А. А., Варваров В. В., Лук'янчиков А. А., Дроль О. Ю.

Застосування технологій цифрового формування й обробки радіолокаційних сигналів надає широкі можливості для впровадження зондувальних радіоімпульсів з різноманітними законами частотної (фазової) модуляції (маніпуляції). З введенням в радіотехнічні системи лінійно-частотно модульованих сигналів розпочалися дослідження щодо зниження максимального рівня бічних пелюсток їх автокореляційних функцій, які не втратили своєї актуальності і на сьогодні. Один з напрямків зниження цього рівня ґрунтується на застосуванні сигналів з нелінійною частотною модуляцією, які складаються з кількох фрагментів. Встановлено, що для уникнення викривлень в результуючий сигнал необхідно вводити компенсуювальні складові, які враховують частотно-фазові спотворення від першого та подальших стиків, а також додаткових приростів фази у самих фрагментах, починаючи з другого.

Дане дослідження присвячено розробленню нової математичної моделі трифрагментного сигналу у складі першого фрагмента з корінь-квадратичною частотною модуляцією та двох наступних фрагментів з лінійною модуляцією частоти. Такий сигнал забезпечує зниження максимального рівня бічних пелюсток у порівнянні з класичним лінійно-частотно модульованим сигналом на 11.43 дБ. Відмінною особливістю цієї математичної моделі є визначення та введення до виразів, які описують другий та третій фрагменти сигналу, нових компенсуювальних складових.

Логіка дослідження обумовлює структуру роботи. Перший її розділ присвячено аналізу відомих публікацій, який свідчить про відсутність робіт за даним напрямком, що обумовлює актуальність та доцільність виконання завдання дослідження, яке сформульовано у другому розділі. У третьому розділі здійснено теоретичне обґрунтування основних положень – визначено особливості виникнення та отримано розрахункові вирази для визначення компенсуювальних складових частотно-фазових спотворень, що виникають на першому та другому стиках, а також у другому та третьому фрагментах сигналу для випадку, коли перший фрагмент має нелінійний закон частотної модуляції, а два наступних – лінійний.

Подальші дослідження планується спрямувати на визначення доцільності та особливостей спільного застосування спектральних і часових віконних функцій під час оброблення радіолокаційних сигналів.

Ключові слова: нелінійна частотна модуляція; математична модель; стрибок миттєвої частоти та фази; автокореляційна функція; максимальний рівень бічних пелюсток